Morphology and Corrosion Behaviour of Zn-Ni-P Thin Films Electrolessly Deposited from Chloride Baths

ANA MARIA POPESCU[1], VIRGIL CONSTANTIN[1]*, MIRCEA OLTEANU[1], VASILE SOARE[2], MARIAN BURADA[2], ELENA IONELA NEACSU[1]*

[1] "Ilie Murgulescu" Institute of Physical Chemistry, 202 Splaiul Independentei, 060021, Bucharest, Romania

[2] National Institute of Research and Development for Non-Ferous and Rare-Metals, 102 Biruintei Blv., 077145, Pantelimon-Ilfov, Romania

Electroless Zn-Ni-P thin film alloys deposits on steel substrate from chloride bath ($ZnCl_2$, $NiCl_2$) containing ammonium chloride as a buffer agent and sodium citrate as a complexing agent were investigated. The effects of deposition conditions (temperature, bath composition, time) on the final deposit composition were studied. It was found that the percentages of zinc and phosphorus in the obtained Zn-Ni-P alloys never reach high values. Some physical characteristics such as morphology and corrosion properties of Zn-Ni-P coatings were assessed. Corrosion tests were done in 3.5 wt.% sodium chloride aerated solution. Corrosion rate values were determined to be 0.1283-0.0297 mm·year^{-1} comparative to 0.2104 mm·year^{-1} for the uncoated steel substrate.The surface analysis of the thin film samples before / after corrosion was performed by X-ray photoelectron spectroscopy (XPS) in an attempt to understand the chemistry of the obtained thin films.

Keywords: Zn-Ni-P thin films, electroless deposition, corrosion; morphology, XPS spectra

When left unprotected, steel will corrode in almost any environment. Historically, cadmium has been extensively used as a barrier coating for steel in aerospace, electrical, and fastener industries owing to its excellent corrosion resistance and other engineering properties [1]. However, cadmium plating is generally done using cyanide baths, which are subject to stringent regulations [2]. Also, cadmium plating presents major disadvantages due to metal toxicity and utilized salts as well as simultaneous discharge of hydrogen ions during the cadmium plating process, making cadmium plating parts to be susceptible of acid provoked brittleness. For these reasons, in the last decades, intense studies and researches were accomplished for finding replacements for cadmium based anticorrosive protection coatings. The most common sacrificial layer replacements for cadmium are zinc and its alloys. Zinc presents a more negative electrode standard potential (E=-0.76 V, measured vs. hydrogen normal electrode), thus being capable of acting as a sacrificial coating for plated steel parts [3]. The dissolution rate of the protective coating was considerably reduced by alloying zinc with other elements (Ni, Co, Fe, etc.) that shifted the standard electrode potential of the alloy to values closer to those of the substrate [4]. Zinc-nickel alloy coatings have been suggested in the literature as replacement for cadmium coating because this alloy provides good corrosion protection on steel [5]. Zn-Ni alloys containing 15-20 wt. % Ni have been shown to possess four times more corrosion resistance than cadmium-titanium deposit [6]. However, due to the high zinc content in the deposit, these alloys have more negative potential than cadmium and hence dissolve rapidly in corrosive environments. Although Ni is nobler than Zn, the co-deposition of Zn-Ni is anomalous and a higher percentage of Zn is present in the final deposit. Several attempts have been made to decrease the anomaly and increase the nickel content either by introducing inert species in the bath or by developing ternary alloys [7-9]. Among these, ternary Zn-Ni-P alloys have a special attention because the addition of 1-5% P leads to a significantly increased corrosion resistance [10-11]. An attractive method for obtaining ternary Zn-Ni-P alloy coatings and for increasing Ni content in the deposited layer is the process of electroless (autocatalytic) reduction of metals that means a chemical deposition (no current use) in the presence of an oxidizing agent. This method was used for obtaining Zn-Ni-P coatings from sulphate and chloride solutions [12]. Electroless deposited Zn-Ni-P thin films have been used as a barrier film on a galvanic Zn or Ni-Zn sacrificial layer in multi-component corrosion protective coatings on steel [13]. The advantage of this barrier film would be a lower electrode potential difference with the underlying steel. Several researches have been carried out to characterize the structure and phase composition of very thin electroless Ni-Zn-P film deposited from ammonium chloride bath [13-17].

The objective of the present work is to investigate some Zn-Ni-P thin film alloys that are electrolessly deposited on steel substrate. The effects of changes in morphology and corrosion resistance of the thin films due to the operating conditions (bath composition and operation parameters) were studied.

Experimental part

Samples preparation

The samples were denoted as ZNP (from 1 to 5). Plating and subsequent corrosion studies were done on carbon steel substrate (symbolized by W) as foils, 50 x 25 mm in size surface area and 0.6 mm in thickness. Table 1 shows the chemical composition of the steel substrate.

Before depositing, a special treatment of the steel samples is necessary because the adherence between the substrate and the coating has favorable consequences on corrosion protection efficiency. The preparation process of the substrate for thin films deposition consisted in the following operations: polishing with abrasive paper of increased granulation; acetone degreasing and rinsing in double distilled water; sample etching, for removing traces

* email: virgilconstantin@yahoo.com, neac_elena@yahoo.com

	Chemical composition (wt. %)				
	C	Si	Mn	Ni	Fe
Steel (W symbolized)	0.0043	0.044	0.41	0.011	99.49

Table 1
CHEMICAL COMPOSITION OF THE STEEL SUBSTRATE

Deposition	Chemical composition (g L^{-1})				
	$ZnCl_2$	$NiCl_2 \times 6H_2O$	$NaH_2PO_2 \times H_2O$	$C_6H_5Na_3O_7 \times 2H_2O$	NH_4Cl
B1 and B2	10	50	50	10	100
B3	10	47	45	10	50
B4	10	47	45	4	26
B5	10	30	40	20	40

Table 2
COMPOSITION OF THE ELECTROLESS DEPOSITION BATH

Sample	Bath	Temperature (° C)	Time (min)	$*t_{steel}$ *at the moment of introduction in the bath (° C)
ZNP 1	B1	85	120	85
ZNP 2	B5	80	60	80
ZNP 3	B4	85	120	80
ZNP4	B3	90	60	20
ZNP 5	B2	75	120	75

Table 3
OPERATION CONDITIONS FOR OBTAINING Zn-Ni-P FILMS

of surface adherent oxide with 50% sulfuric acid solution at a temperature of 50-60°C for 1-2 min, followed by washing with double distilled water.The experimental setup for electroless deposition consisted in a thermo-resistant vessel of 600 cm^3 volume and a magnetic heater-stirrer. The used baths were prepared with double distilled water and analytical grade reagents (Merck). The Zn-Ni-P thin films were deposited from solutions containing zinc chloride ($ZnCl_2$), nickel chloride ($NiCl_2$. $6H_2O$), sodium citrate ($C_6H_5Na_3O_7$. $2H_2O$) and ammonium chloride (NH_4Cl, as buffer agent). Sodium hypophosphite ($NaHPO_2$. H_2O) was used as a reducing agent for the electroless process and also as a phosphorus source in the deposited films. *p*H value was maintained at 9.5 during the deposition process by addition of sodium hydroxide (NaOH). These baths were chosen after some preliminary investigations on the spontaneous de-composition of the solutions and to optimize the plating rate. Samples of Zn-Ni-P films with different compositions were obtained by varying the concentration of nickel chloride and sodium hypophosphite, temperature of the both bath and steel foil (when it was introduced in the bath) and also immersion time.

The experimental conditions for obtaining the Zn-Ni-P thin film samples are given in tables 2 and 3.

Characterization of thin films

The SEM micrographs and elemental analysis data of the steel substrate were obtained using a Philips XL-30-SEM-TMP scanning electron microscope provided with energy dispersive X-ray analysis (EDX) equipment.

For increasing the accuracy degree of the elemental distribution, the EDX analysis was performed in various points situated along a diagonal of the steel parts. The accuracy of the measurements for the equipment used was rated as ±0.1 wt. %. Surface morphologies of the Zn-Ni-P samples after the electrochemical corrosion tests were observed using an optical metallographic microscope (mm0011000m-Microscope Inc. SUA) with 40-800 magnification range. Surface analysis of the coating samples before and after the corrosion process was performed by X-Ray Photoelectron Spectroscopy (XPS) using a "Quantera SXM-Japan" equipment. The X-ray source was Al K_α radiation (1486.6 eV), and the energy resolution is estimated at 0.65 eV by the full width at half maximum (FWHM) of the $Au4f_{7/2}$. The acquired peaks in XPS spectrum were further deconvoluted with a commercial computer program (PHI Multipack version 9.1.0.9.). The deconvoluted peaks were identified by reference to an XPS data base [18]

Corrosion testing

The corrosion behaviour of the electroless Zn-Ni-P thin film alloys was investigated in quiescent aerated 3.5 wt. % NaCl solution, which had a *p*H=6.483 (measured with the pH-meter "IonoLab *p*H-730", Germany). Tafel potentiodynamic polarization curves were plotted as specific electrochemical procedure, which permitted the establishing of the corrosion potential (E_{corr}), corrosion current (i_{cor}) and polarization resistance [12, 19]. The corrosion studies were carried out at 30°C using a Princeton Applied Research model PARSTAT 2273 potentiostat/galvanostat with a "Power Corr" corrosion software. A thermostated glass cell was used, in which the working electrode was the steel Zn-Ni-P covered (with a surface of 1 cm^2), the auxiliary electrode was a platinum plate (Radiometer electrode, model M-241PT) and the reference electrode was a saturated calomel electrode (SCE, Radiometer-model 451). To begin the experiments the sample was introduced into the NaCl aggressive solution and was allowed to reach equilibrium, which usually took around 20 min. In our experiments the open circuit potential (OCP) was measured after 30 min. The polarization resistance (R_p) was measured using potentiodynamic linear polarization at ± 20 mV vs. E_{OCP} [20]. Tafel polarization experiments were performed with constant scan rate of 0.166 mVs^{-1}, the potential being shifted within ±250 mV *vs.* E_{OCP}. When plotting the polarization curves we take into account that prolonged anodic polarization might give rise to changes at the surface roughness which would imply parallel translation of the Tafel slopes. This effect was eliminated by first plotting the cathodic branches and then the anodic ones.

Results and siscussions

Morfological characterization studies

The Zn-Ni-P deposits obtained on steel are bright or semi-bright grey in appearance. The SEM micrographs of the samples ZNP1-ZNP5 are presented in figure 1 and show that the surface morphology is homogenous and not porous, with rounded formations. In general, the substrate surface defects determine the growing morphology; at

higher magnifications an uniform covering with the deposition film is revealed with local developments as spheres with a "cauliflower" aspect. Depending on the deposition process parameters, in the case of the very thin film, one can observe some cracks and rifts uncovered yet because of the lower film thickness. The surface rifts lead also to an apparent tendency of oriented growing, probably determined by the local different kinetics of the deposition mechanism along these rifts.

From the dispersive X-ray analyses (EDX) it was found that the chemical composition of Zn-Ni-P film is almost the same in different zones. Figure 2 shows the EDX spectra of the studied samples, where only peaks for Zn, Ni, P and Fe elements appear, demonstrating the purity of the coating; obviously the Fe peak are due to the substrate interference.

The mechanism of the electroless deposition using sodium hypophospite as the reducing agent has been well-established in the literature and the deposition mechanism was explained by the mixed potential theory [12]. According to this theory, the electroless process occurs at a potential where the net current is zero, so that the current due to the anodic reaction (oxydation of hypophosphite) is equal to the sum of the cathodic currents (reduction of Ni, Zn, P and H_2). The oxidation of hypophosphite species occurs *vs.* SCE at -0.75 V, reduction of nickel ions occurs at -0.53 V and reduction of Ni ions is accompanied by the H_2 evolution reaction at -0.28 V. However, when Zn is added to the bath, the codeposition of Zn with Ni-P deposition occurs at -1.043V *vs.* SCE [21]. In fact,using bath for only Zn-Ni electroless deposition it has been previously observed that Zn is codeposited and the formation of Ni rich phase in Zn-Ni alloys occurs at more positive potentials [22]. This suggests that a similar phenomenon occurs in the electroless deposition of Zn-Ni-P alloys.

As it was already established that Zn^{2+} ions act as inhibitors for the electroless Ni-P process, our objective was to increase the Zn content in the final Zn-Ni-P deposit (but not higher than 20%), taking care of having in the same time a high Ni content [23]. In order to explain the process occurring during the electroless Zn-Ni-P deposition from alkaline electrolytes a model was developed taking into account a model proposed for electroless process in sulfates media [24]. According to Pourbaix diagrams [25], both Zn^{2+} and Ni^{2+} ions will precipitate as $Zn(OH)_2$ and $Ni(OH)_2$, respectively, at *p*H>7.0. For the deposition to be carried out in alkaline conditions, it is necessary the use of complexing agents to prevent the metal ions from spontaneous precipitation. In our case the complexing agent used was sodium citrate. In the presence of ammonia the following complex ions and precipitates are formed:

$$Zn(OH)_2 + 4NH_3 \rightarrow Zn(NH_3)_4^{2+} + 2OH^- \quad (1)$$

$$Ni(OH)_2 + 6NH_3 \rightarrow Ni(NH_3)_6^{2+} + 2OH^- \quad (2)$$

$$Zn^{2+} + 2OH^- \rightarrow Zn(OH)_2 \quad (3)$$

$$Ni^{2+} + 2OH^- \rightarrow Ni(OH)_2 \quad (4)$$

Zinc and nickel complexes can be reduced to deposit as Zn-Ni alloy with the release of ammonia. In the presence of sodium hypophosphite the following reactions of oxidation of hypophospite, reduction to phosphorus, zinc and nickel, and hydrogen evolution will take place as following:

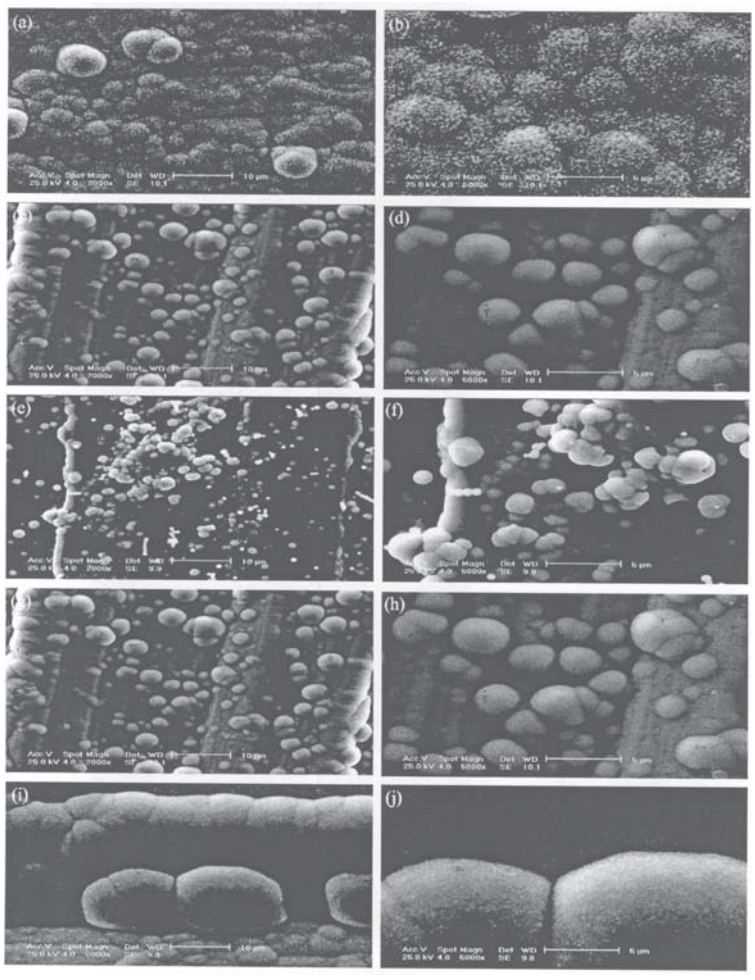

Fig.1 SEM micrographs (with magnifications x2000 and x5000) for Zn-Ni-P thin films deposited on steel. Samples: ZNP1(a,b); ZNP2 (c,d); ZNP3 (e,f); ZNP4 (g,h); ZNP5 (i,j)

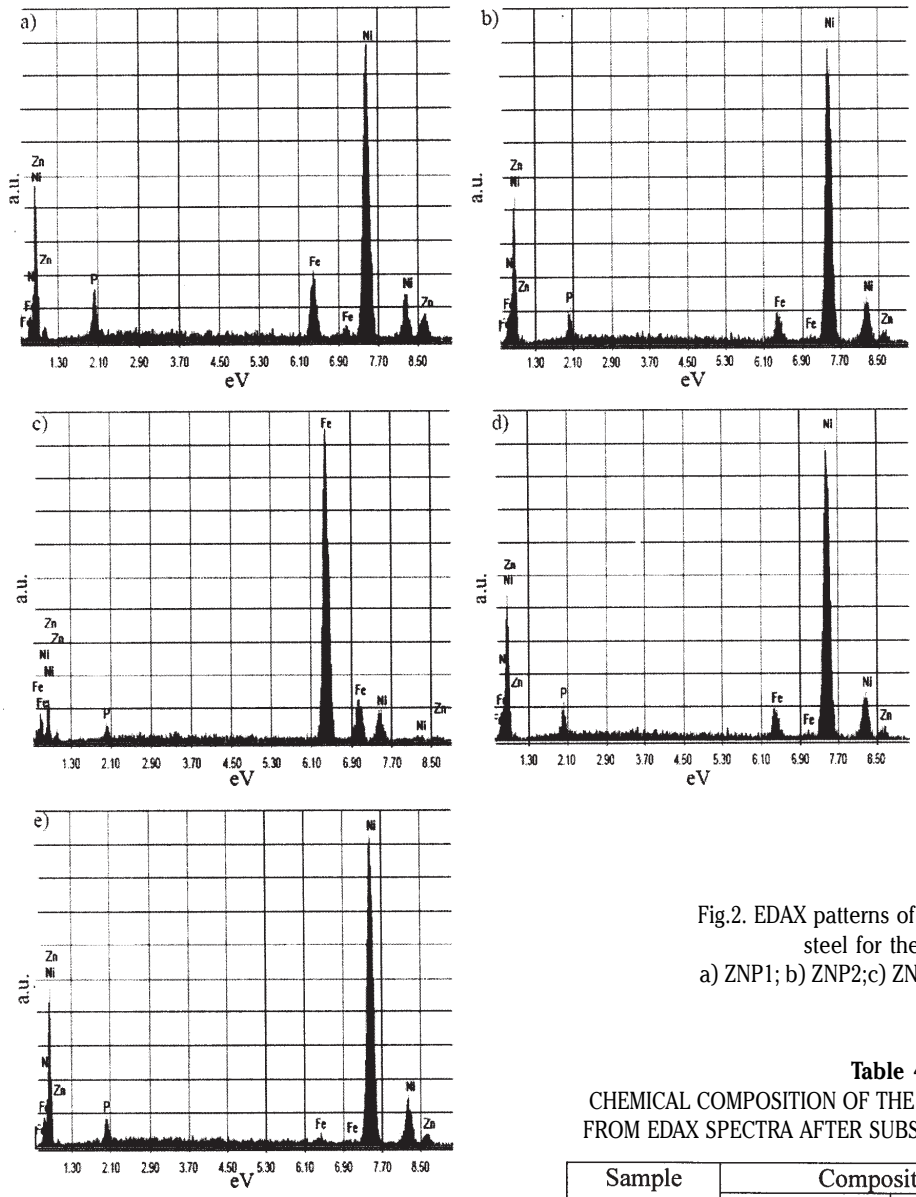

Fig.2. EDAX patterns of Zn-Ni-P thin films on steel for the samples:
a) ZNP1; b) ZNP2;c) ZNP3; d) ZNP4; e) ZNP5

$$H_2PO_2^- + H_2O \xrightarrow{catalytic\ surface} H_2PO_3^- + 2H^+ + 2e^- \quad (5)$$

$$2H_2PO_2^- + H^+ + e^- \rightarrow P + HPO_3^- + H_2O + H_2 \quad (6)$$

$$Zn(NH_3)_4^{2+} + 2e^- \rightarrow Zn + 4NH_4 \quad (7)$$

$$Ni(NH_3)_6^{2+} + 2e^- \rightarrow Ni + 6NH_3 \quad (8)$$

$$2H^+ + 2e^- \rightarrow H_2 \quad (9)$$

The composition of the electroless deposited Zn-Ni-P films is presented in table 4. The obtained results of EDX analysis proved a high content of nickel (73.51-91.60 wt. %) in Zn-Ni-P alloy deposits. As for the contents of zinc and phosphorous, these are very low (4.84-12.84 wt. % Zn and 3.56-13.65 wt. % P, respectively).

As the composition of Zn^{2+} ions in the deposition bath was constant, we assumed that the most important role was played in the bath by the Ni^{2+} content. The variation in the composition of the obtained Zn-Ni-P coatings as a function of nickel chloride concentration in the bath is presented in figure 3. In this figure there are presented only four dependences by considering that the bath for samples ZNP1 and ZNP5 has the same nickel chloride concentration and only ZNP5 is representative. It was found that the Zn and P contents in the alloy decrease with increasing the Ni ion concentration in the bath.

Table 4
CHEMICAL COMPOSITION OF THE ZNP SAMPLES DETERMINED FROM EDAX SPECTRA AFTER SUBSTRACTING THE Fe CONTENT

Sample	Composition analysis, wt%		
	Zn	Ni	P
ZNP 1	7.81	86.74	6.13
ZNP2	12.84	73.51	13.65
ZNP3	5.44	90.92	3.64
ZNP4	5.44	90.91	3.64
ZNP5	4.84	91.60	3.56

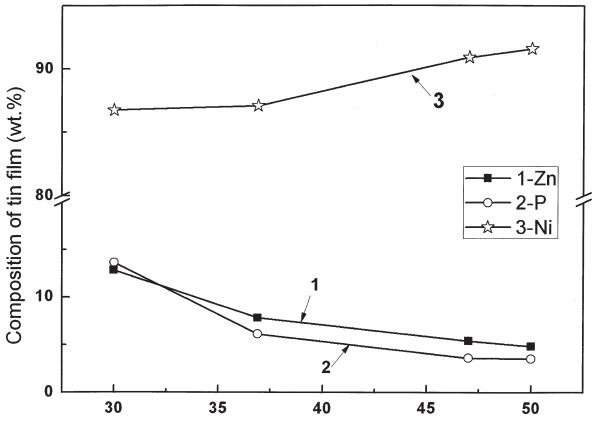

Fig.3 Variation in the Zn, Ni and P contents of the coatings with $NiCl_2$ x $6H_2O$ concentration in the deposition bath

Sample	W	ZNP1	ZNP2	ZNP3	ZNP4	ZNP5
E_{OCP} (V)	-0.539	-0.334	-0.469	-0.509	-0.448	-0.534
R_p (KΩ cm^2)	3.911	27.195	24.202	11.365	9.563	1.861

Table 5
VALUES OF OPEN CIRCUIT POTENTIAL AND POLARIZATION RESISTANCE FOR BARE STEEL AND Zn-Ni-P THIN FILMS

Corrosion behaviour

In order to evaluate the appropriate ion concentrations in the bath for optimal thin films of Zn-Ni-P to be obtained, the corrosion resistance of the studied samples was evaluated. Comparative potentiodynamic polarization studies for uncoated carbon steel and carbon steel coated with Zn-Ni-P alloy of different compositions were carried out in order to evaluate the corrosion rate in 3.5 wt. % NaCl solution. The corroded surface was observed visually and micrographically for the identification of formation of any white/red rust on the coating. Literature show that when Zn-Ni alloy coatings are exposed to salt solutions, zinc hydroxide is found to form as corrosion product [26]. This product is known as "white rust" which bears the indication of corrosion. The same phenomenon we noticed when Zn-Ni-P is exposed to salt solution. The open circuit potential (OCP) was evaluated for quantitative evaluation. For a given electrolyte solution, the OCP is dependent on the characteristics of resulted oxide, such as oxide thickness, composition, conductivity, structure, etc. At the initial time of immersion in the NaCl corrosive environment the studied alloys present OCP potential values varying from -0.539V for uncoated steel (W) sample to -0.534 V for ZNP4 sample and to -0.334 V for ZNP1 sample. Most rapid evolution of potential occurrs during the first 7-10 minutes of immersion, while further potential evolution becomes slower and OCP values do not change significantly, having a slow monotonous shift towards more positive values. The initial OCP values are listed in table 5.

As can be seen, the values of OCP for various Zn-Ni-P alloys depend strongly of the zinc content in the alloy, but all OCP values of the studied Zn-Ni-P samples exhibited more positive potentials than carbon steel substrate (-0.539V). The time evolution of OCP indicates that the passive film is thinning and consequently becomes vulnerable toward anion penetration of Cl^- ions. Also, we noticed slight oscillations of OCP in time. We assumed that these OCP oscillations may result from chemical interactions between chloride ions and the structured passive film. As in all samples the nickel content is higher than 73 %, this behaviour may be considered as depending strongly on zinc and phosphorous content in the alloy.

Linear polarizations studies were carried out to estimate the polarization resistances (R_p) for corrosion of steel and of the various coatings studied. The resulting potential *vs.* current density curves show a liniar dependence. The slope of the linear part of these plots yields the polarization resistance values listed also in (table 5). The R_p values obtained for Zn-Ni-P films are also higher as compared to the steel substrate (R_p=3.9114 kΩ cm^2), which means that these samples will have lower corrosion rate than the steel substrate. However, the sample ZNP5 is an exception as it was found to have a lower polarization resistance than bare steel. Tafel polarization curves were also employed to evaluate the effect of the Zn-Ni-P coatings on the corrosion resistance of carbon steel substrate. Figure 4 shows the potentiodynamic polarization curves for the studied samples. The corrosion current density i_{corr} was determined either by extrapolating the cathodic and anodic Tafel lines to E_{corr} or according to the Stern-Geary equation [18]. The corresponding corrosion parameters were obtained from the Tafel polarization curves using "Power Corr" soft. The penetration index as corrosion rate CR (in millimeters per year) is obtained by using the following equation:

$$CR = C \frac{EW}{\rho} \frac{i_{corr}}{A} \quad (10)$$

where:

EW is equivalent weight of the sample in g, A is sample area in cm^2;

ρ is density in g cm^{-3},;

C is a constant C=3.268 . 10^3, if i_{corr} is in amperes.

The plots indicate that all Zn-Ni-P thin films have better corrosion protective properties than the steel substrate. All samples show a positive shift in the corrosion potential (with the exception of sample ZNP3) and decrease corrosion current. In other words, the studied thin films have lower chemical activity than steel substrate and hence possess better chemical stability in the aggressive environment.

From figure 4 we can conclude that for the sample ZNP1 a passivation process may occur rapidly. The determined values of corrosion potential, corrosion current density and corrosion rate are listed in table 6. Data from table 6 show that E_{corr} values are shifted positively and i_{corr} values decreased

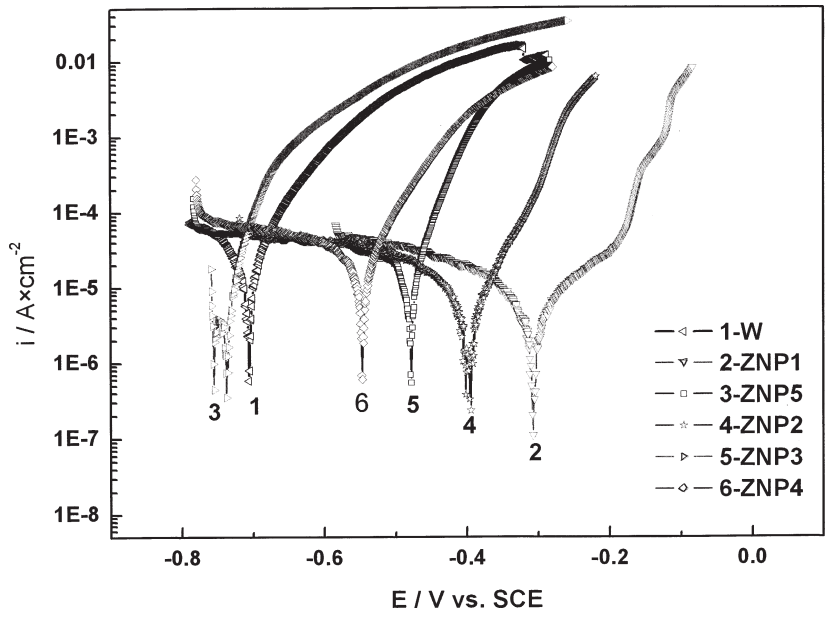

Fig. 4. Comparative Tafel graphs of steel (W) and ZNP 1-5 samples in 3.5 wt. % NaCl solution at 30°C

Sample	$i_{corr} \times 10^4$ (A cm^{-2})	$E_{corr\ (ZCP)}$ (V *vs.* SCE)	CR (mm year^{-1})
W	0.0896	-0.7061	0.2104
ZNP1	0.0126	-0.3076	0.0297
ZNP2	0.0188	-0.3972	0.0442
ZNP3	0.0272	-0.546	0.0638
ZNP4	0.0547	-0.4791	0.1283
ZNP5	0.0777	-0.7378	0.4158

Table 6
CORROSION PARAMETERS MEASURED AND CALCULATED FOR THE STEEL SUBSTRATE AND THE STUDIED THIN FILMS IN 3.5WT% NaCl SOLUTION AT 30°C

* i_{corr} = corrosion current; $E_{corr(ZCP)}$ = corrosion potential$_{(i=0)}$; CR = corrosion rate.

Sample	ZNP1	ZNP3	ZNP5
Estimated/calculated film thickness [μ]	14.8 / 14	9.6 / 9	30.8 / 36
Thin film adherence	Good adherence	Moderately adherence	Imperfect adherence

Table 7
THICKNESS AND ADHERENCE OF THIN FILMS

with the increase of Zn content in the alloy, although literature indicates a high zinc content for corrosion protection [12]. The obtained results for CR presented in table 6 are in good agreement with the R_p values from table 5. It is very clear that all studied samples with the exception of ZNP5, have corrosion protective properties and the best behaviour is for ZNP1. Electrochemical data indicate that the sample ZNP5 is totally unsatisfactory in terms of corrosion resistance and therefore this, sample is non-recommended in terms of corrosion protection; this could be also observed by visual introspection of this sample before corrosion as the Zn-Ni-P thin film was not completely and uniformly deposited.

The SEM images of the same sample show the presence of big spheres with a "cauliflower" aspect (fig. 1e), which permitted the formation of pores and could generate massive corrosion.

Micrographic introspection of the samples after corrosion

A micrographic study was performed on some of the samples and the results are presented in figure 5. Looking at the micrographic images one can clearly understand

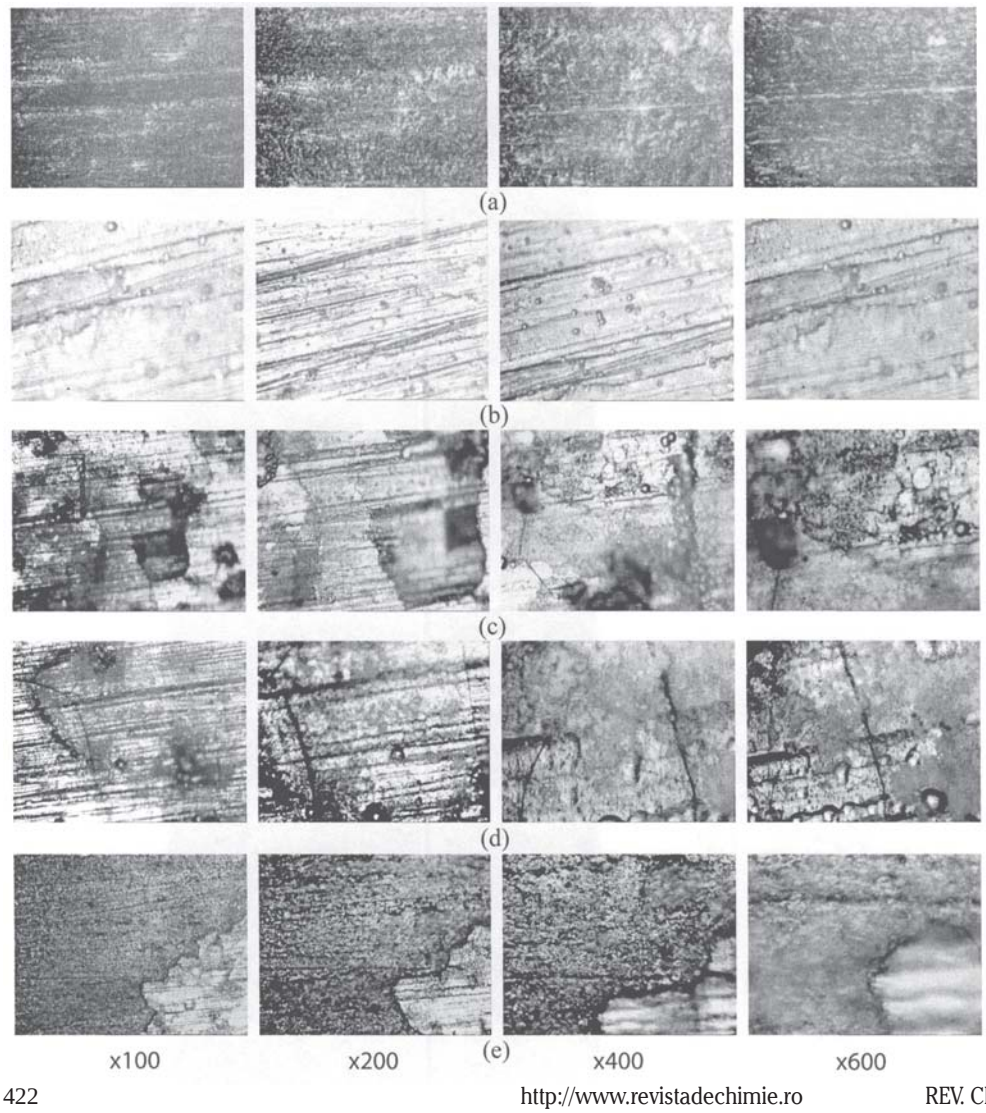

Fig.5 Micrographs of sample surfaces after corrosion experiments: a) ZNP1; b) ZNP2; c) ZNP3; d) ZNP4; e) ZNP5

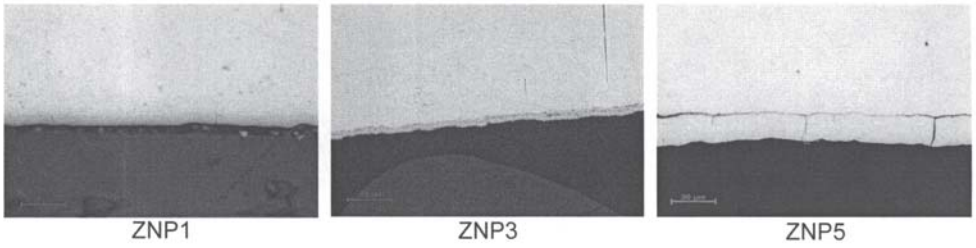

Fig.6 Micrographs of cross-sections of the samples ZNP1(a), ZNP3 (b) and ZNP5 (c)

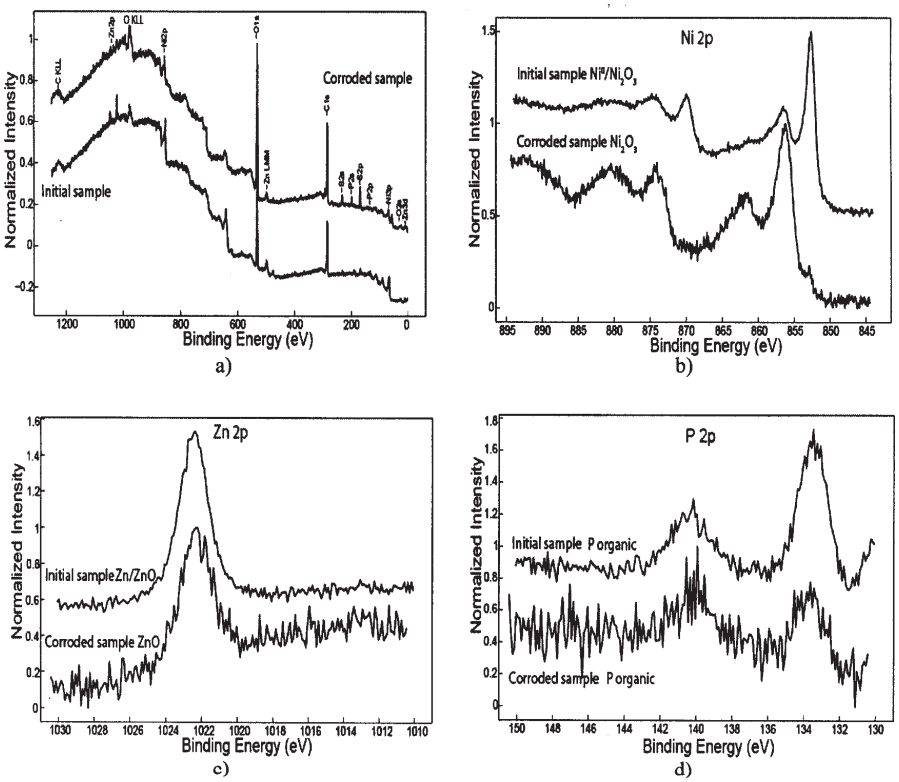

Fig.7. Superimposed XPS survey spectra (a) and the deconvoluted XPS spectra of Ni 2p (b), Zn 2p (c) and P 2p(d) for the initial and corroded ZNP1 sample.

the low corrosion protection efficiency for the samples ZNP4 and ZNP5 which both present after the corrosion test a destroyed structure with cracks (probably resulted from producing an internal stress) and big rust deposits. Oppositely, samples ZNP1 and ZNP2 present almost none structural modifications of the surface which is well correlated with the good corrosion rates of these samples. A special behaviour was registered for ZNP3, which although has good corrosion rate, has not a good enough aspect after short-term corrosion test (fig. 5c). We consider that in case of some samples with inconsistent results, an important cause of a low corrosion rate obtained could be the not very well substrate preparation before electroless deposition of Zn-Ni-P thin films.

Some of the steel samples coated with ZNP thin films were weighted in order to determine the amount of deposited alloy and the thickness of the films using the equation:

$$h = \frac{G}{2\rho S} \quad (11)$$

where:

h- film thickness[μm];

G-weight of the alloy deposit [g];

ρ -density of the Zn-Ni-P alloy [~8.5g cm^{-3}];

S-surface area of the steel sample [~8cm^2].

The obtained results are presented in table 7 and figure 6 that shows the micrographs of cross-section of these samples, explaining exactly the good or bad adherence of the thin films.

X-ray Photoelectron Spectrosopy (XPS) analysis was also used to determine the chemical states of the elements present on the surface of the Zn-Ni-P thin film alloys deposited on steel substrate before and after the corrosion process. The characteristic thickness detected by XPS method for the deposited layers is found in the range of (5-7.5) nm, whereas the quantitative analysis revealed the presence of C, O, Zn, Ni and P elements. Figure 7a shows comparatively the survey XPS spectra for the initial/coroded ZNP1 sample.We have to mention that all XPS measurements on the studied samples gave similar spectra, which display the characteristic XPS transitions of the detected elements on the surface, respectively Zn, Ni, P as principal elements and C,O,S as contaminants elements. The high resolution photoelectron spectra of the most prominent XPS transitions (Zn 2p, Zn LMM, Ni 2p and P 2p) were obtained by deconvolution (fig.7 b,c,d). The spectra for Zn LMM is similar with that for Zn 2p. From the XPS measurements it is clearly that Zn and Ni are present in the corroded samples as oxides, while the P element is present as an organic compound (corrosion product) due to the presence of the sodium citrate in the bath.

Conclusions

Comparative morphological and corrosion studies carried out on a number of five covered samples and bare steel substrate demonstrated the efficiency of corrosion protection for electroless deposits consisting in Zn-Ni-P alloy. Taking into account the corrosion rate and morphological aspect we can conclude that one of the best procedures for obtaining high protective Zn-Ni-P thin films is the electroless plating process at 80-85°C, operating with a bath containing $ZnCl_2$, $NiCl_2$ and NaH_2PO_2 for immersion times of about 60-120 min. The optimum composition of the Zn-Ni-P films from the point of view of

corrosion properties is that the high nickel content (>73.5%) and ~8-13 % Zn and ~6-13% P content in the deposit.

Acknowledgements: Support of the Partnership Romanian Research Program (PNCDI2), CORZIFILM project nr.72-221/2008-2011, bilateral project "AR-FRBCF-2011" and "EU (ERDF) and Romanian Government" that allowed for acquisition of the research infrastructure under POS-CEEO2.2.1 project INFRANANOCHEM-Nr.19/ 01.03.2009, is gratefully acknowledged.

References

1. BALDWIN, K.R., SMITH, C.J.E., Trans. Inst. Met. Finish., 74, 1996, p.202.
2. SAFRANEK, W.H., Plat. Surf. Finish., 84, 1997, p.45.
3. SWATHIRAJAN, S., J. Electrochem. Soc., 133, 1986, p.671.
4. SHORT, N.R., ZHOU, S., BENNIS, J.K., Surf. Coat. Technol., 79, 1996, p.218.
5. ASHUR, A., SHARON, J., KLEIN, I.E., Plat. Surf. Finish., 83, 1996, p.58.
6. LIN, Y.P., SELMAN, J.R., J. Electrochem. Soc., 140,1993, p.1299.
7. VEERARAGHAVAN, B., KIM, H., HARAN, B., POPOV, B., Corrosion, 59, 2003, p.1003.
8. VEERARAGHAVAN, B., KIM, H., HARAN, B., POPOV, B., Electrochim. Acta, 49, 2004, p.3143.
9. GANESAN, P., KUMARAGURU, S.P., POPOV, B.N., Surf. Coat. Technol., 201, (2006), p.3658.
10. ZHOU, Z., O'KEEFE, T.J., Surf. Coat. Technol., 96, 1997, p.191.
11. VALOVA, E., GEORGIEV, I., ARMYANOV, S., DELPLANCKE, J.L., J. Electrochem. Soc., 148, 2001, p.C266.
12. VEERARAGHAVAN, B., HARAN, B., KUMARAGURU, S.P., POPOV, B., J. Electrochem. Soc., 150 2003, p.B131.
13. SCHLESINGER, M., MENG, X., SNYDER, D., J. Electrochem. Soc., 138, 1991, p.406.
14. BOUANANI, M., CHERKAOUI, F., FRATESI, R., J. Appl. Electrochem., 29, 1999, p.637.
15. BOUANANI, M., CHERKAOUI, F., CHERKAOUI, M., BELCADI, S., FRATESI, R., ROVENTI, G. J., J. Appl. Electrochem., 10, 1999, p.1171.
16. VALOVA, E., GEORGIEV, I., ARMYANOV, S., DELPLANCKE, J.L., TACHEV, D., TSACHEVA TS., DILLE J., J. Electrochem. Soc., 148, 2001, p.C266.
17. POPESCU, A.M., CONSTANTIN, V., SOARE, V., TIRCOLEA, M., OLTEANU, M., Rev. Chim. (Bucharest), **62**, no. 9, 2011, p.899.
18. MOULDER, J. F., STICKLE, W. F., SOBOL, P. E., BOMBEN, K. D., Handbook of X - ray Photoelectron Spectroscopy, Publish ULVAC-PHI Inc., Japan 1995.
19.REVIE, R.W.: Uhlig's Corrosion Handbook, sec.ed., John Wiley & Sons Inc., 2000.
20. STERN, G., GEARY, A. L., J. Electrochem. Soc., 104, 1957, p.56.
21. ROVENTI, G., FRATESI, R., DELLA GUARDIA, R.A., ABRUCA, G., J. Appl. Electrochem., 30, 2000, p.173.
22. FABRI, F.J.M., BARCIA, O.E., MATTAS, O.R., WIART, R., J. Electrochem. Soc., 144, 1997, p.3449.
23. LEUKONIS, J., Zh. Prikl. Khim., 51, 1978, p.1797.
24. VEERARAGHAVAN, B., KIM, H., POPOV, B., Electrochim. Acta., 49, 2004, p.3143.
25. POURBAIX M.: Atlas of Electrochemical Equilibria in Aqueous Solutions, Pergamon Press, 1966.
26.RAHMAN, M.J., SEN, S.R., MONIRUZZAMAN, M., SHOROWORDI, K.M., J. Mech. Eng., Tran., 40, 2009, p.9

Manuscript received: 29.11.2012